Effect of initial infection size on a network susceptible-infected-recovered model

G. Machado and G. J. Baxter
Department of Physics & I3N, University of Aveiro, Campus Universitário de Santiago, 3810-193 Aveiro, Portugal

(Received 18 March 2022; revised 22 June 2022; accepted 30 June 2022; published 21 July 2022)

We consider the effect of a nonvanishing fraction of initially infected nodes (seeds) on the susceptible-infected-recovered epidemic model on random networks. This is relevant when the number of arriving infected individuals is large, or to the spread of ideas with publicity campaigns. This model is frequently studied by mapping to a bond percolation problem, in which edges are occupied with the probability p of eventual infection along an edge. This gives accurate measures of the final size of the infection and epidemic threshold in the limit of a vanishingly small seed fraction. We show, however, that when the initial infection occupies a nonvanishing fraction, f, of the network, this method yields ambiguous results, as the correspondence between edge occupation and contagion transmission no longer holds. We propose instead to measure the giant component of recovered individuals within the original contact network. We derive exact equations for the size of the epidemic and the epidemic threshold in the infinite size limit in heterogeneous sparse random networks, and we confirm them with numerical results. We observe that the epidemic threshold correctly depends on f, decreasing as f increases. When the seed fraction tends to zero, we recover the standard results.

DOI: 10.1103/PhysRevE.106.014307

I. INTRODUCTION

Compartmental epidemic models provide a powerful mathematical tool for predicting and understanding the spread of contagions. In these models, the population is divided into several compartments, representing different states of individuals with respect to the disease. Perhaps the most well known and one of the simplest compartmental models is the susceptible-infected-recovered (SIR) model [1], which describes the spreading of contagions, such as diseases, from which individuals recover with immunity. An important generalization of such models is to consider the spread taking place on a heterogeneous contact network [2]. Most individuals begin in the susceptible state, while a small number, the seeds, are initially in the infected state. Infected individuals may pass the infection to susceptible neighbors, who then become infected. Infected individuals may in turn recover, after which their state no longer changes. Here we consider the infection to occur along each edge linking an infected to a susceptible individual with some rate β, while infected individuals recover at a rate α. This process is summarized in Fig. 1.

The infection may spread to only a small number of individuals, or across a significant portion of the network. The process ends when no more infected nodes remain, so that all sites are either recovered or still susceptible.

This remains a dynamic and active field of research, with researchers considering numerous aspects of network disease spreading models [3], including, for example, the effects of network structure [4], degree correlations [5], and heterogeneous transmission rates [6]. Such models, and more complex variations of them, form the basis of efforts to model and predict the SARS-CoV-2 epidemic [7,8].

Usually, theoretical models use the initial condition of a minute fraction of infected individuals, [2–5,9], or a single infection [6,10–12], with all others initially being susceptible. However, some works have considered the effect of nontrivial initial conditions. Dynamic equations explicitly accounting for a large initial infection were considered in [13]. The effect of the particular location of initial infections was considered in [14] and [15]. Recently, studies of the SIR process in well-mixed populations in the critical regime have shown that the initial fraction f of infected individuals may have a significant effect on the progression of the epidemic [16–18].

The authors of Ref. [19] considered the effect of a nonvanishing initial infection size on the epidemic threshold in random regular networks, finding, as we do, that the epidemic threshold is sensitive to the value of f, especially at small values. They showed that this behavior arises because the infection clusters originating from different seeds percolate before the cluster from any single seed can form a giant component. They used a master equation approach, which leads to several coupled equations in the regular graphs studied. While in principle this method could be extended to more heterogeneous graphs, the number of coupled equations would increase rapidly, making the approach impractical. We have instead developed a self-consistency equation approach, which allows us to immediately consider heterogeneous random graphs. This results in only two coupled equations, which can easily be solved, regardless of the complexity of the degree distribution.

The effect of initial seed fraction has also been considered in the bootstrap percolation and k-core processes [20,21]. The application of such models is not limited solely to diseases, as very similar models can trace the spread of ideas [22] and other applications, from communication to finance [23].

FIG. 1. Schematic illustration of the SIR process. Each individual is in one of the three states—susceptible (S), infected (I), or recovered (R)—at each point in time. Infected individuals transmit the infection to susceptible neighbors with a rate β per unit time. Susceptible individuals transition to the infected state upon receiving the infection. Note that the label β indicates this rate parameter, which does not correspond to the transition rate of susceptible individuals to the infected state. Infected individuals transition to the recovered state with rate α per unit time. After an individual is recovered, their state can no longer change.

In these cases, too, the initial seeding of the contagion may be (intentionally) widespread, representing media coverage, political campaigns, or advertising.

Our aim in this paper is to explore the effect of the fraction, f, of randomly chosen initial infections on the SIR epidemic process occurring on a heterogeneous random network. We show that the usual approach of mapping the epidemic size to the network giant component in a bond percolation process [24] is inadequate for a nonvanishing initial seed fraction. This is because there is no longer a one-to-one correspondence between occupied edges in the percolation mapping, and disease transmission in the SIR model. We propose instead to measure the giant component of infected individuals within the original contact network. This gives an unambiguous interpretation and correctly reflects the effect of the initial seed fraction. We derive self-consistency equations that allow us to calculate the size of this giant component and the epidemic threshold exactly in uncorrelated random networks in the large-size limit. These theoretical results are in good agreement with simulations even for moderately sized networks. In this formulation, the threshold now depends on the seed fraction f. This enables, for example, the identification of the size of the initial infection required to provoke a large outbreak. Importantly, small changes in f can produce significant changes in this threshold, so careful consideration of initial conditions is necessary for an accurate prediction of epidemics. We confirm the observation made in [19] for regular random graphs, namely that the finite clusters of infections caused by each seed percolate before any individual seed can infect a finite fraction of the network, as illustrated in Fig. 2.

The paper is organized as follows. In Sec. II we specify the SIR model that we use, and we provide the general equations for calculating node infection probabilities. In Sec. III we introduce our proposed measure of the outbreak size, and we show how it can still be calculated based on the percolation mapping, with careful adaptation. In Sec. IV we show how the epidemic threshold may be determined. In Sec. V we summarize how the threshold varies with respect to the parameters f and p (the probability that an infected individual infects a susceptible neighbor before recovering) using the example of Erdös-Rényi networks. Conclusions are presented in Sec. VI.

II. THE MODEL

We now describe the SIR model in detail. We consider a system of N individuals, each represented by a different vertex

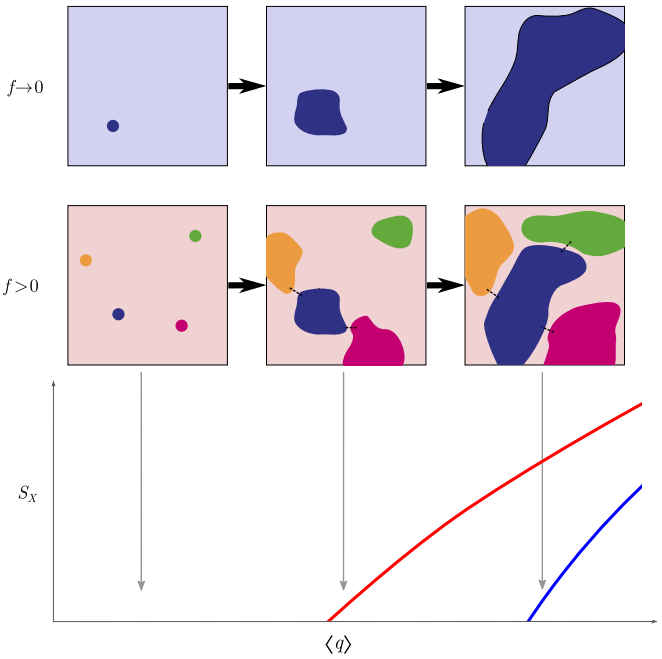

FIG. 2. Stylized illustration of the evolution of the system as the density of connections increases. In the limit $f \to 0$ (top row), the cluster of infections from a seed node grows and eventually forms a giant component beyond a critical threshold, indicated by the cluster connecting more than one border of the region, in the rightmost panel. For larger f (second row), the clusters from multiple seeds grow and eventually meet each other, forming a giant component within the contact network at a lower threshold (middle panel) before any individual cluster forms a giant component. At the bottom of the figure, we also sketch the size of the giant component S_X as a function of network density (mean degree $\langle q \rangle$) for $f \to 0$ [lower (blue) curve] and $f > 0$ [upper (red) curve]. Each panel corresponds to the position in the plot indicated by the vertical arrows.

of a contact network. Each individual can be in one of three states at a given time: susceptible, infected, or recovered. A susceptible node can only evolve to the infected state, and an infected node can only evolve to the recovered state. Once a node is recovered, it can no longer leave this state. Thus the system evolves as shown in Fig. 1.

At the start of the process ($t = 0$), a fraction f of individuals, chosen uniformly at random, are set to the infected state. We will refer to these nodes as the seeds. All remaining individuals are initially susceptible. In the limit of large system size, a finite number of seeds corresponds to $f \to 0$. (Note that in finite systems, the smallest realizable value of f is actually $1/N$.) Considering finite values for f has important implications for the size of the epidemic and how it should be measured.

Each infected node transmits the infection to each of its susceptible neighbors (who then become infected), independently, with rate β per unit time. Also, each node in the infected state moves to the recovered state at rate α per unit time. (This corresponds to an exponential infected lifetime distribution, which we have chosen merely for the sake of simplicity. One may choose any other distribution without affecting the analysis.) Thus, the network in the infinite time

limit will be constituted solely of susceptible and recovered nodes.

We assume a large, sparse, uncorrelated random contact network. Such a network is defined by its degree distribution $P(q)$, where q is the node degree, with mean degree $\langle q \rangle$. The relative fraction of cycles in the network vanishes as the system size tends to infinity. That is, the network is locally treelike in the large size limit. This allows us to write self-consistency equations for all the relevant quantities.

The usual approach is to map this problem to a bond percolation problem [24]. Let us define p to be the probability that an infected individual ever transmits the infection to a given susceptible neighbor before recovering. In a continuous time formulation of this process, this probability is

$$p = \frac{\beta}{\alpha + \beta}. \tag{1}$$

One may also consider a discrete-time process; see Appendix B.

Now, starting from the seed nodes, the infection traverses each edge with probability p. We can consider the edges for which this happens as being occupied with probability p. The nodes that can be reached by following occupied edges are the ones that will eventually become infected. Thus all the nodes in any connected cluster in the bond percolation problem that contains at least one seed node will be infected, and hence will be recovered at the end of the process. Thus the fraction of nodes that are infected (and end up recovered) is equal to the fraction of nodes in connected clusters in the bond percolation problem that contain at least one seed.

Using the locally treelike property of the network, one can then calculate the probability that a randomly selected node is recovered at the end of the process by writing a self-consistent equation

$$S_Z = f + (1 - f) \sum_{q=1}^{\infty} P(q)[1 - (1 - Z)^q]. \tag{2}$$

The first term represents the probability that the node is a seed, which is infected from the start. The second term gives the probability that the node is a nonseed node and has at least one edge leading to an occupied subtree containing at least one seed node. The probability, Z, that an edge leads to such a subtree can be calculated recursively by solving

$$Z = p\left[1 - (1 - f) \sum_{q=1}^{\infty} \frac{qP(q)}{\langle q \rangle}(1 - Z)^{q-1}\right]. \tag{3}$$

The first term represents the probability of following an occupied edge and encountering a seed. The second term regards the probability of following an occupied edge and meeting a nonseed node, of any degree, which has at least one other edge (not counting the edge along which we arrived at the node) which satisfies the same condition. These equations depend on the assumption that the transmission of the disease in each edge is independent of the others, which is valid under the treelike approximation.

We emphasise that S_Z does not correspond to the size of any connected cluster, but is simply the fraction of nodes that are recovered at the end of the process (having at some time been infected). As such, it does not display any phase transition.

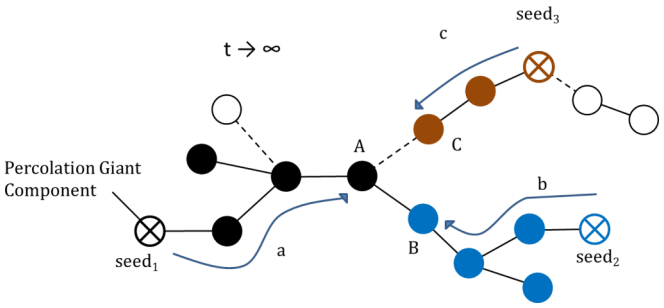

FIG. 3. Example of how nodes infected from different infection paths can be included/excluded from the percolation giant component due to ambiguous edges. Seed nodes (initial infection) are marked with a cross, and infected nodes are shaded. Arrows indicate the chains of infections. Occupied edges in the percolation mapping are shown as solid lines, unoccupied edges are dashed. Node A received the infection via a chain of infection starting from Seed 1, node B from that starting at Seed 2, and node C from that starting at Seed 3. Seed 1 has a connection leading to the giant component of the percolation network. Neither the occupied edge between A and B nor the unoccupied edge between A and C ever passed the infection, in either direction, yet the cluster of nodes with infection originating in Seed 2 is connected to the percolation giant component by a path of occupied edges, while the cluster with infection originating in Seed 3 is not.

III. MEASURING THE SIZE OF THE EPIDEMIC

One may then ask, when does a large outbreak—an epidemic—appear? Typically in network SIR models, one looks for the appearance of a giant component in the percolation mapping [9]. This approach gives an unambiguous result when the initially infected nodes form a vanishing fraction of the network ($f \to 0$). In this limit, the existence of an occupied edge in the percolation problem represents infection in clusters where there is a seed. Then the giant component in the bond percolation problem, if it exists, differs from the entire set of infected nodes only by a small number of infected nodes in finite clusters. One finds a sharp epidemic threshold in the control parameter (network mean degree, say) above which an epidemic appears.

When $f > 0$, this no longer holds true, and several difficulties arise with the percolation mapping treatment. The nonvanishing density of seeds means that occupied edges do not necessarily correspond to the path of infection as there may be multiple such paths leading from different seeds to the same node. Furthermore, clusters of infections originating from individual seeds may be arbitrarily included or excluded from the percolation giant component, depending on the presence or absence of a connecting occupied edge. This means that the size of the percolation giant component no longer matches the epidemic size. Furthermore, as a finite fraction of the network is always infected, there is no longer a sharp transition in the total fraction of infected nodes. Finally, the percolation giant component size does not change with f. Some of these ambiguities are illustrated in Fig. 3.

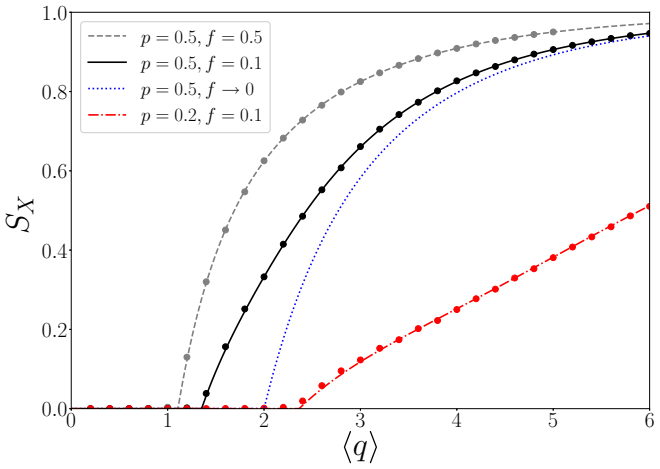

FIG. 4. Size S_X of the epidemic, measured as the size of the giant component of infected nodes within the original contact network, as a function of mean degree $\langle q \rangle$ for several combinations of seed fraction, f, and transmission probability, p, as indicated in the legend. The giant component appears at an epidemic threshold that decreases with increasing f for the same value of p. For smaller p, the threshold is delayed and the epidemic is smaller. The theoretical curve for the limit $f \to 0$ corresponds to the usual treatment of the SIR model on a network. Note that for finite graphs, the smallest realizable value is $f = 1/N$. Markers show numerical results for Erdös-Rényi networks with $N = 10^5$ nodes, averaged over 10 realizations. Curves are theoretical results obtained from Eqs. (15)–(20).

Our main consideration when addressing this problem is coherence. One should either maintain only edges across which the infection was transmitted (severing both links B–A and A–C in the example shown in Fig. 3), or include all adjacent infected components as part of the same cluster (keeping both of the edges in the example). The first choice would result in a separate connected component for each seed node, creating numerous finite clusters, which would be insufficient to describe the general behavior of the system, and would make comparison of results for different values of f difficult (Ref. [25], pp. 62 and 63). Instead, we choose to measure the size of the giant component of recovered nodes (that have been infected at some time) connected by the original edges of the full contact network, that is, ignoring the status of edges as having been used in infecting or not. In the remainder of this section, we will simply refer to this as the "giant component." Note that this much more closely resembles the situation one might find oneself in when dealing with a real epidemic, in which the infections are known but the path of infection may not be. As we will see, we can still calculate the size of this giant component using the edge occupation probability p, by careful consideration of the probability that a node is recovered, and that it belongs to the giant component. We find that the second-order phase transition at the emergence of the giant component is retained, but that the threshold and size of the giant component now depend on the seed fraction f. The giant component is also larger, as some finite clusters connected only by unoccupied edges are now included; see Fig. 4.

The percolation mapping is still useful for calculating the probability that a given node is ever infected. We therefore look for a giant component within the original contact network, considering only nodes that have been infected (recovered nodes).

The fraction, S_X, of nodes that belong to the giant component is equal to the probability that a randomly selected node has at least one connection to the giant component (of recovered nodes within the contact network in the final state), and has at least one connection leading, via a path of occupied edges, to a seed node. This probability obeys the following equation:

$$S_X = f \sum_{q=1}^{\infty} P(q) \sum_{l=1}^{q} \binom{q}{l} X^l (1-X)^{q-l} + (1-f) \sum_{q=1}^{\infty} P(q) \times \left[1 - (1-Z)^q - \sum_{l=1}^{q} \binom{q}{l} Y^l (1-X-Y)^{q-l} \right], \quad (4)$$

where Z is as defined above. We define X to be the probability that, starting from a node that is recovered in the final state, and following a random edge, we encounter a neighbor that connects to the giant component via one of its remaining edges (whether occupied or not in the percolation mapping). Having at least one such connection thus guarantees that a node belongs to the giant component. We also define Y to be the probability that by following an occupied edge from a recovered node, one meets a neighbor that is recovered, but that does not connect to the giant component via any of its other edges.

The first term in Eq. (4) represents the probability that the node is itself a seed, in which case we just need the condition that it has at least one connection to the giant component, which occurs for each edge with probability X. We construct the second term, for the case when the node is not a seed, negatively by subtracting from 1 the probability of never being infected $[(1-Z)^q]$, and further subtracting the probability that it does become infected, but that any path leading to a seed node does not lead to the giant component (Y), and neither do any of the other edges. This is necessary because, unlike in the standard percolation mapping, the configurations counted by X are no longer a subset of those corresponding to Z, as we also include the possibility of connections via unoccupied edges.

To find X and Y, we construct a pair of coupled self-consistency equations, accounting for the configurations illustrated in Fig. 5. If the node encountered upon following an edge (leading from a recovered node) is a seed, or if the edge we follow is occupied (so that the node at its end could have been infected from the node we started from), we require simply a further connection to the giant component, cases 1) and 2) in the figure, respectively. The final possibility contributing to X, case 3), requires that the node encountered has at least one ongoing connection of the type corresponding to Z, as well as at least one corresponding to X. As these are partly overlapping, it is easiest to calculate this term negatively, subtracting probabilities that lead to finite subtrees. This requires the probability Y, which accounts for configurations satisfying Z but not X.

These terms and their probabilities are described in detail in Appendix A. After some simplification, we arrive at the

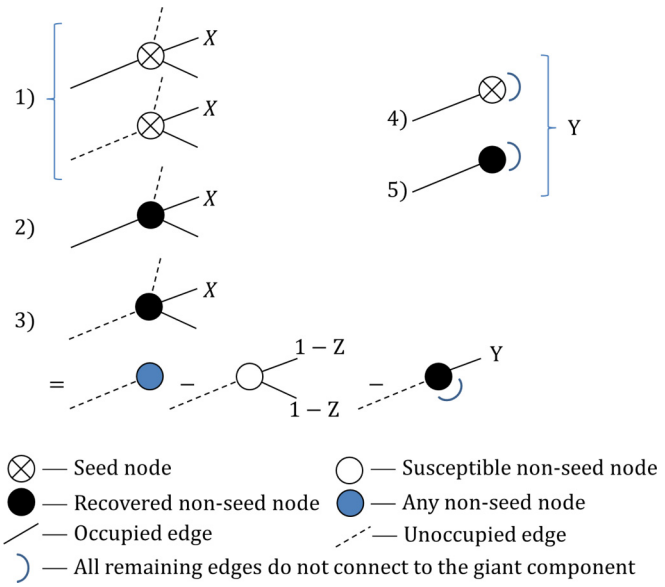

FIG. 5. All the possible cases contributing to the probability X, and those contributing to the probability Y. The probability X accounts for when, on following an edge, we encounter a node that was infected at some time, and has at least one further connection satisfying the same condition (indicated by the symbol X in the figure). The different terms, representing different configurations contributing to X, are labeled 1), 2), and 3). Case 3) can be described negatively by using the probability Y that a node is infected but does not connect to the giant component. The terms contributing to Y are labeled 4) and 5). The probabilities corresponding to these numbered terms are described in Appendix A.

following coupled equations:

$$X = \sum_{q=1}^{\infty} \frac{qP(q)}{\langle q\rangle}\{[1-(1-X)^{q-1}] + (1-p)(1-f)[(1-X-Y)^{q-1}-(1-Z)^{q-1}]\} \quad (5)$$

and

$$Y = p\sum_{q=1}^{\infty} \frac{qP(q)}{\langle q\rangle}[(1-X)^{q-1}-p(1-f)(1-X-Y)^{q-1}]. \quad (6)$$

Using Eq. (2), we can simplify Eq. (4) as

$$S_X = S_Z - \sum_{q=0}^{\infty} P(q)[(1-X)^q + (1-f)(1-X-Y)^q]. \quad (7)$$

One may also write the fraction of recovered nodes that do not belong to the giant component, S_Y. Nodes in this situation are either seeds that do not connect to the giant component via any of their edges, or nonseed nodes with at least one neighbor which transmitted the disease to it, but none of its neighbors connect to the giant component, giving

$$S_Y = \sum_{q=0}^{\infty} P(q)(1-X)^q - (1-f)\sum_{q=0}^{\infty} P(q)(1-X-Y)^q \quad (8)$$

so that

$$S_X = S_Z - S_Y, \quad (9)$$

with S_Z given by Eq. (2).

IV. EPIDEMIC THRESHOLD

Clearly when $X \ll 1$, then $S_X \ll 1$, and specifically $S_X = 0$ when $X = 0$. Looking at Eqs. (5) and (6), we can see that the $X = 0$ (the probability of connecting to the giant component being zero) is always a solution (with Y becoming equal to Z). A second solution for X eventually appears, marking the emergence of a giant epidemic. To calculate the point at which this happens (the critical point), we assume that the giant component appears continuously from zero, and we linearize Eq. (5) around the critical point:

$$X = \frac{\langle q(q-1)\rangle}{\langle q\rangle}X - (1-p)(1-f)G_2(1-Z)(X-\delta) + O(X^2), \quad (10)$$

where

$$G_n(x) \equiv \sum_{q=0}^{\infty} \frac{P(q)}{\langle q\rangle}\frac{d^n}{dx^n}x^q \quad (11)$$

and $\delta \equiv Z - Y$, which we assume to be small. In fact, $\delta = 0$ below the transition and is very small just above it.

Making a similar expansion for Y in orders of X allows us to write an expression for δ in terms of X:

$$\delta = \frac{p\frac{\langle q(q-1)\rangle}{\langle q\rangle} - p(1-f)G_2(1-Z)}{1-p(1-f)G_2(1-Z)}X. \quad (12)$$

Using Eq. (12) to eliminate δ, eliminating a factor of X, and rearranging, we arrive at the condition for the epidemic threshold:

$$1 = \frac{\langle q(q-1)\rangle}{\langle q\rangle} - (1-p)(1-f)G_2(1-Z) \times \left[\frac{1-p\frac{\langle q(q-1)\rangle}{\langle q\rangle}}{1-p(1-f)G_2(1-Z)}\right]. \quad (13)$$

For details of this derivation, see Appendix D.

Notice that this is not an explicit equation with respect to the model parameters p (itself a function of the rates α and β), f, and the degree distribution $P(q)$ and its moments. Instead, one must solve this equation simultaneously with Eq. (3). For a specific degree distribution, one may obtain a closed-form condition for the critical point; see the following section. Equation (13) may be used to obtain the critical point with respect to p, for example holding all other parameters fixed, but also fixing p (i.e., α and β) to find the minimal number of nodes that have to start in the infected state for the emergence of a giant epidemic.

Including further terms in the expansion of Eq. (5), we can determine that X, and hence the epidemic size S, grows linearly above the epidemic threshold:

$$S \approx (p-p_c)^{\beta} \quad (14)$$

with $\beta = 1$, as for the standard percolation transition. See Appendix D for the derivation of this result.

V. RESULTS FOR ERDÖS-RÉNYI NETWORKS

To illustrate the dependence of the epidemic on the various parameters, we now consider the specific case of Erdös-Rényi networks, whose degree distribution tends to Poisson in large systems, $P(q) = \frac{e^{-\langle q\rangle}\langle q\rangle^q}{q!}$. In this case, Eqs. (2), (7), and (8) become

$$S_Z = 1 - e^{-\langle q\rangle Z}, \tag{15}$$

$$S_X = S_Z - e^{-\langle q\rangle X}[1 - (1-f)e^{-\langle q\rangle Y}], \tag{16}$$

$$S_Y = e^{-\langle q\rangle X}[1 - (1-f)e^{-\langle q\rangle Y}], \tag{17}$$

while Eqs. (3), (5), and (6) become

$$Z = p[1 - (1-f)e^{-\langle q\rangle Z}], \tag{18}$$

$$X = (Z - Y)\left(\frac{1-p}{p}\right) + p(1 - e^{-\langle q\rangle X}), \tag{19}$$

$$Y = pe^{-\langle q\rangle X}[1 - (1-f)e^{-\langle q\rangle Y}], \tag{20}$$

$$\delta = \frac{\langle q\rangle XZ}{1 - \langle q\rangle(p - Z)}. \tag{21}$$

We illustrate the solution of Eq. (16), which depends on the simultaneous solution of Eqs. (18)–(20), in Fig. 4. We see that the size of the epidemic, as well as the threshold at which it emerges, depends on the seed fraction f when other parameters are held equal.

With a Poisson degree distribution as described, we have

$$G_2(1 - Z) = \langle q\rangle e^{-\langle q\rangle Z}, \tag{22}$$

which, substituting into Eq. (13), gives us the condition for the critical point of an Erdös-Rényi graph:

$$1 = \langle q\rangle + \frac{(1-p)}{p}\langle q\rangle(Z - p)\left[\frac{1 - p\langle q\rangle}{1 + \langle q\rangle(Z - p)}\right], \tag{23}$$

where we have used Eq. (18) to obtain the last line. Remembering that Z is a function of mean degree $\langle q\rangle$, one can obtain the threshold $\langle q\rangle_c$ numerically by solving Eq. (23) together with Eq. (18).

Figure 6 shows how $\langle q\rangle_c$ changes with p for different values of f. We can see that the critical points for the same p decrease with increasing f as a greater initial presence of seeds facilitates the formation of the giant component. At the critical point, the finite clusters of infections from each seed connect to one another (via unoccupied or occupied edges), together forming a giant component even though none of the seeds individually has infected a finite fraction of the network. This is illustrated in a stylized way in Fig. 2. Similarly, the overall epidemic size is larger for larger f for equal values of all other parameters. See also Fig. 4. If we were to use the standard method of measuring the size of the percolation giant component, we would only obtain the limiting $f = 0$ curve. It is also observable that, especially for small values, small changes in small values of f have a large effect on the critical threshold, highlighting the importance of f on the system's evolution.

In the limit $f = 1$, all nodes are seeds, and the epidemic threshold corresponds to the site percolation threshold

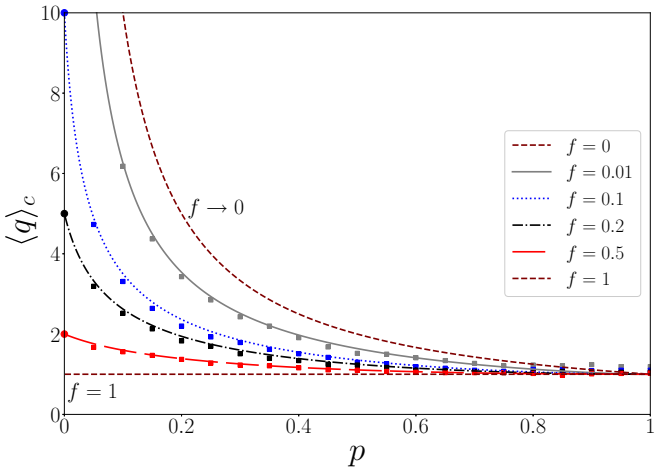

FIG. 6. Epidemic threshold for the mean degree, $\langle q\rangle_c$, as a function of p for several values of f, as indicated in the legend. Curves represent the theoretical calculation for, from top to bottom, $f = 0.01$, 0.1, 0.2, 0.5, and 1. The upper and lower dashed lines represent the theoretical calculations for the limits $f \to 0$ and $f = 1$, respectively. Circular markers indicate the limiting value as $p \to 0$. Square markers represent critical points measured from discrete-time simulations on Erdös-Rényi networks of $N = 10^4$ nodes using 1000 realizations. Critical points were identified as the peak value of susceptibility; see Appendix C.

$\langle q\rangle_c = 1$, irrespective of the value of p. In the limit $p \to 0$, when the seed fraction is not zero, the critical point does not diverge (as it does for $p \to 0$ with $f \to 0$), because the seeds eventually percolate by themselves, at the point $\langle q\rangle = 1/f$, indicated by the circular markers in the figure. In the limit $p = 1$, the giant component of the epidemic corresponds to the giant connected component of the contact network, as all the infected nodes transmit the disease to all their neighbors.

In Fig. 7, we show the minimal fraction of seeds sufficient for an outbreak to occur (which we define as f_{crit}) as a function p for several values of the mean degree, $\langle q\rangle$. Naturally, as the probability of infection, p, increases, the minimal fraction of seeds sufficient for an outbreak diminishes. The superior horizontal dashed line represents the case of $\langle q\rangle = 1$, above which there is no giant epidemic, as there is no giant component of nodes in the contact network in the first place. In the limit $\langle q\rangle \to \infty$, f_{crit} tends to zero, even for $p \to 0$, as the number of connections between nodes compensates for the lack of seeds and infectiousness. At the limit $p = 1$, the threshold corresponds to the percolation threshold of the seeds. At the horizontal axis ($f \to 0$), we find the epidemic threshold for the standard SIR model for each value of $\langle q\rangle$.

Finally, Fig. 8 shows how the threshold on the network's parameter evolves with f for a fixed p. One may observe that this figure is very similar to Fig. 6. These similarities result due to two reasons: first, both p and f are variables whose increase (decrease) facilitates (hinders) the appearance of an epidemic; second, there is a symmetry between the limiting curves in both figures. The lower limit corresponds to the percolation threshold with respect to $\langle q\rangle$ of the substrate contact network when all edges are occupied ($p = 1$, Fig. 8) or all nodes are occupied as seeds ($f = 1$, Fig. 6). Meanwhile the

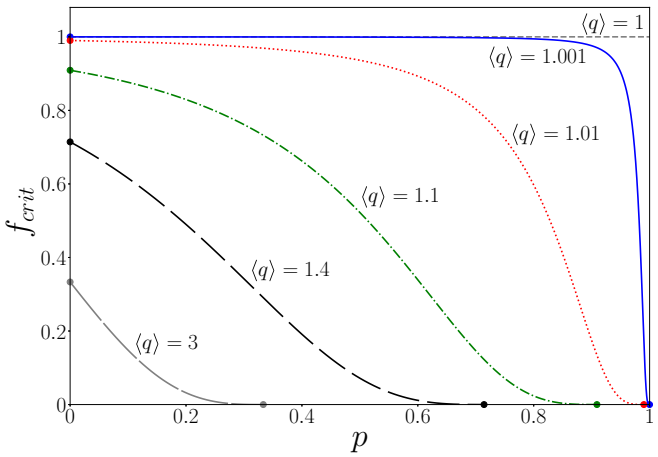

FIG. 7. Epidemic threshold for f as a function of p for several values of mean degree $\langle q\rangle$. Solid lines represent the theoretical prediction for the minimal fraction of seeds sufficient for an outbreak to occur, at each value of $\langle q\rangle$. The upper dashed line (gray) represents the theoretical prediction for the limit $\langle q\rangle \to 1$, the minimal value of $\langle q\rangle$ for the appearance of a giant component in the network. The markers indicate the point at which each line intercepts with each axis.

upper limit corresponds to percolation of the seeds for a given value of $\langle q\rangle$ ($p \to 0$, Fig. 8) or percolation due to occupied edges ($f \to 0$, Fig. 6).

VI. CONCLUSIONS

In this paper, we have presented a generalization of the well known SIR model of disease spreading on a network to consider the effect of allowing the fraction of initially infected nodes, f, to be nonvanishing.

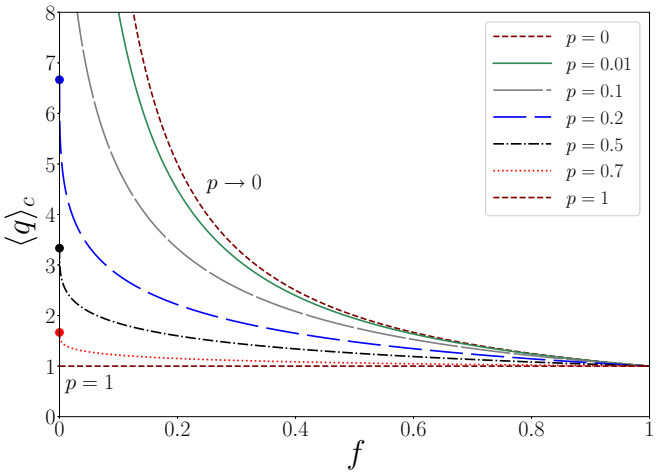

FIG. 8. Theoretical calculation of the epidemic threshold $\langle q\rangle_c$ as a function of f for several values of p as indicated in the legend. The upper and lower dashed lines represent the theoretical values for the limits $p \to 0$ and $p = 1$, respectively. Circular markers indicate the interception between the theoretical lines and the vertical axis at $f = 0$.

The size of the epidemic in the SIR model is usually calculated by mapping the process to a bond percolation problem, and the initial condition is usually taken to be either a single infection, or infection of a vanishingly small fraction of the network ($f \to 0$ in the large system size limit). In this case, the occupied edges correspond to the paths of infection through the contact network. The size of the percolation giant component then gives the exact expected outbreak size, also allowing the determination of the epidemic threshold.

We found, however, that allowing the initial fraction of infected nodes, f, to be larger leads to a disconnection between the size of the percolation giant component and the epidemic size. The percolation mapping calculation shows no dependence on f. Worse, clusters of recovered nodes may be included or excluded from the giant component arbitrarily, and occupied edges no longer correspond perfectly to disease infection. Thus the calculated giant component does not accurately represent the size of the epidemic nor the paths of infection through the network.

To resolve this problem, we instead measure the giant component of recovered nodes in the original contact network, keeping all edges. This mimics the situation one might encounter in a real epidemic: the social contacts are known, but the exact path of the infection may not be, when there are multiple contacts. We extended the usual self-consistency equations to show how the size of this giant component can be calculated, starting from the percolation mapping. This was done by separating the probability that the node encountered upon following a random edge is infected, from the probability that it connects to the giant component. We find that the expected size of the epidemic and the epidemic threshold both now correctly depend on the initially infected fraction, f. In particular, we find that a larger initial infection (larger f) means that the epidemic threshold is reached sooner (lower epidemic threshold) with respect to the other parameters. When other parameters are kept equal, a larger value of f corresponds to a larger epidemic size. Near $f = 0$, the threshold is highly sensitive to the value of f, showing that an accurate determination of initial conditions is crucial to the correct modeling of the evolution of an epidemic and correct estimation of other model parameters.

We studied the model on Erdös-Rényi random networks as an example of sparse random graphs. The results will be qualitatively the same for any uncorrelated random networks with finite first and second moments of the degree distribution. In fact, our method can be directly generalized to consider, for example, nearest-neighbor degree correlations, arbitrary infection lifetime distributions, or heterogeneous transmission rates, without significantly increasing the difficulty of the analysis. In other words, all the results already found for the $f \to 0$ limit can easily be extended to nontrivial initial conditions using our method.

Our generalization of the SIR model is also relevant to the spread of opinions, ideas, or technology, in which, for example, active campaigning produces an initial seed fraction that is not of negligible size. We believe that this work contributes to the general understanding of this fundamental model, and it shows that a careful consideration of nontrivial initial conditions should be one element included in more

realistic generalizations of the model and its application to specific situations.

ACKNOWLEDGMENTS

We warmly thank Alexander Goltsev for helpful discussions and suggestions for improving the manuscript. This work was support by the i3N associated laboratory LA/P/0037/202, within the scope of the projects UID-B/50025/2020 and UID-P/50025/2020, financed by national funds through the FCT/MEC. This work was also supported by National Funds through FCT, I. P. Project No. IF/00726/2015. G.M. was supported by FCT PhD Research Scholarship SFRH/BD/08794/2020.

APPENDIX A: SELF-CONSISTENCY EQUATIONS FOR THE PROBABILITIES X AND Y

We define X to be the probability that, starting from a node that is recovered in the final state, and following a random edge, we encounter a neighbor that connects to the giant component via one of its remaining edges (whether occupied or not in the percolation mapping). The possible cases in which this can happen, also illustrated in Fig. 5, are as follows:

1) The edge is either occupied or unoccupied in the percolation mapping, and the node we meet is a seed, which connects to the giant component by one of its other edges. The probability for this to occur is

$$f\sum_{q=2}^{\infty}\frac{qP(q)}{\langle q\rangle}\sum_{l=1}^{q-1}\binom{q-1}{l}X^{l}(1-X)^{q-1-l}. \tag{A1}$$

2) The edge is occupied, the node we meet is not a seed, but it connects via one of its remaining edges to the giant component. Notice that the node we meet necessarily ends up recovered, since we are defining X as coming from a recovered node. This has the probability

$$p(1-f)\sum_{q=2}^{\infty}\frac{qP(q)}{\langle q\rangle}\sum_{l=1}^{q-1}\binom{q-1}{l}X^{l}(1-X)^{q-1-l}. \tag{A2}$$

3) The edge we are following is unoccupied, the node we meet is not a seed, but it became infected via a different node (i.e., different from the parent one), and it connects to the giant component.

This term is difficult to construct, since it is no longer a subset of the cases of Z. To solve this, we consider the possibilities that, upon following an unoccupied edge, one meets a nonseed node that does *not* connect to the giant component, and then we subtract them from 1. The only cases in which this happens are if either the nonseed node we meet was never infected (all its ongoing edges are cases of $1-Z$), or it was infected but none of its ongoing edges connects to the giant component. This last possibility corresponds to having at least one ongoing connection that corresponds to Y, while all the others which are not Y are also not X. Here Y is the probability that, on following an occupied edge, one meets a neighbor that transmitted to it the disease, but that does not belong to the giant component. This is a subset of the cases of Z. Thus, combining the two cases, term 3) will read

$$(1-p)(1-f)\sum_{q=2}^{\infty}\frac{qP(q)}{\langle q\rangle}\Bigg[1-(1-Z)^{q-1} -\sum_{l=1}^{q-1}\binom{q-1}{l}Y^{l}(1-X-Y)^{(q-1-l)}\Bigg]. \tag{A3}$$

Finally, we need to write the equation for Y. This configuration can happen in two ways, by following an occupied edge that does one of the following:

4) Leads to a seed, but the seed does not connect to the giant component, with probability

$$pf\sum_{q=1}^{\infty}\frac{qP(q)}{\langle q\rangle}(1-X)^{q-1}. \tag{A4}$$

or

5) Leads to a nonseed, which is recovered but which does not connect to the giant component. This requires at least one further connection of a type corresponding to Y, and those that are not Y must also not be X. Probabilistically, this term reads

$$p(1-f)\sum_{q=2}^{\infty}\frac{qP(q)}{\langle q\rangle}\sum_{l=1}^{q-1}\binom{q-1}{l}Y^{l}(1-X-Y)^{(q-1-l)}. \tag{A5}$$

Since all the cases that construct X and Y are independent of each other, we can simply sum their probabilities to obtain

$$X = 1) + 2) + 3), \tag{A6}$$

$$Y = 4) + 5), \tag{A7}$$

where numbers represent the terms described in the correspondingly numbered paragraphs above. Simplifying the resulting equations, we obtain Eqs. (5) and (6).

APPENDIX B: PERCOLATION MAPPING FOR CONTINUOUS AND DISCRETE TIME

Consider the edge connecting an infected node to a susceptible neighbor. The mapping of the contagion process to bond percolation is given by the probability p that the infected node ever infects its susceptible neighbor via this edge [24]. Here we show how p may be obtained both for a continuous-time and discrete-time formulation. Once this value is known, all the results given in the main text are valid for either case.

Given transmission rate β and recovery rate α, the probability that the infection occurs in a very short time interval δt is given by

$$\beta\delta t(1-\alpha\delta t). \tag{B1}$$

The probability that it occurs in a second interval of equal length is, including the probability that it did not occur in the first interval,

$$\beta\delta t(1-a\delta t)(1-a\delta t)(1-\beta\delta t). \tag{B2}$$

Continuing, the probability that the infection occurs in the interval $(t, t+\delta t)$ and not before (where, without loss of generality, we set the time at which the infected node became

infected as $t = 0$) is

$$P_t = \beta\delta t(1-\alpha\delta t)[(1-\alpha\delta t)(1-\beta\delta t)]^{t/\delta t}. \tag{B3}$$

To obtain the continuous time limit, we take $\delta t \to 0$, obtaining

$$P(t)dt = \beta dt e^{-\alpha t} e^{-\beta t}, \tag{B4}$$

where we have changed to a probability density function $P(t)$.

Integrating $P(t)$ over all times, we obtain the probability that a node ever transmitted the disease before it recovered, p:

$$p = \int_0^\infty e^{-\alpha t} e^{-\beta t} \beta dt = \frac{\beta}{\alpha+\beta}. \tag{B5}$$

For the discrete-time formulation, we return to Eq. (B3) and fix the time interval $\delta t \equiv \Delta t$. The probabilities of infection, b, and recovery, a, in a single interval are

$$a = 1 - e^{-\alpha\Delta t}, \tag{B6}$$

$$b = 1 - e^{-\beta\Delta t}. \tag{B7}$$

We then sum P_t over all time intervals to obtain

$$p = \sum_{i=1}^{\infty} b(1-a)[(1-a)(1-b)]^{i-1} = \frac{b(1-a)}{a+b(1-a)}, \tag{B8}$$

where $i = t/\Delta t$.

APPENDIX C: NUMERICAL SIMULATIONS

Simulation results shown in the figures were generated using discrete-time simulations, by choosing single-step infection probability b and recovery probabilities a corresponding to the desired value of p. Correspondence to a continuous time formulation can be found by choosing a value for Δt and using Eqs. (B6) and (B7).

In simulations with discrete time, the order of checking for recovery of transmission becomes important. In our case, we checked for each infected node's recovery first, before they could attempt to transmit the contagion to their neighbors, thus a factor of $1-a$ multiplying with b appears, ensuring that each infected node does not recover in the same time step it transmits the agent. Notice that we recover Eq. (B5) from Eq. (B8) when $\Delta t \to 0$.

The epidemic threshold is identified numerically by looking for the peak susceptibility, defined as

$$\chi = \frac{\langle S_X^2 \rangle}{\langle S_X \rangle^2}, \tag{C1}$$

which has no system size dependence; see Ref. [26] for a discussion of this definition. In simulations S_X is measured as the size of the largest connected component of recovered nodes at the end of the simulation.

APPENDIX D: CALCULATION OF THE CRITICAL EXPONENT β

Let us define

$$G_n(x) \equiv \sum_q \frac{P(q)}{\langle q \rangle} \frac{d^n}{dx^n} x^q. \tag{D1}$$

Then

$$G_1(1) = 1, \tag{D2}$$

$$G_2(1) = \frac{\langle q(q-1) \rangle}{\langle q \rangle}, \tag{D3}$$

$$G_1(1-Z) = \sum_q \frac{qP(q)}{\langle q \rangle}(1-Z)^{q-1}, \tag{D4}$$

$$G_2(1-Z) = \sum_q \frac{qP(q)}{\langle q \rangle}(q-1)(1-Z)^{q-2}, \tag{D5}$$

and so on. Terms of this sort appear frequently in our equations, so at times it will be useful to write them in terms of G_n. It is also useful to see how these may be expanded in terms of a small perturbation to the parameter Z:

$$G_1(1-Z_c-\Delta) \approx G_1(1-Z_c) - G_2(1-Z_c)\Delta + \frac{1}{2}G_3(1-Z_c)\Delta^2 - \cdots \tag{D6}$$

and

$$G_2(1-Z_c-\Delta) \approx G_2(1-Z_c) - 2G_3(1-Z_c)\Delta + \cdots \tag{D7}$$

and so on. We may then rewrite the main equations in terms of G_n:

$$X = [t]1 - G_1(1-X) - (1-p)(1-f)[G_1(1-Z) - G_1(1-X-Y)], \tag{D8}$$

$$Z = p[G_1(1) - (1-f)G_1(1-Z)], \tag{D9}$$

$$Y = p[G_1(1-X) - (1-f)G_1(1-X-Y)]. \tag{D10}$$

It is clear that when $X = 0$, $Y = Z$.

Remembering that $\delta = Z - Y$, subtracting Eq. (D10) from Eq. (D9) gives

$$\delta = p[1 - G_1(1-X)] - p(1-f) \times [G_1(1-Z) - G_1(1-X-Y)]. \tag{D11}$$

Let p_c be the critical value of p, at which point Z takes the value Z_c. Writing $p = p_c + \epsilon$ and $Z = Z_c + \Delta$, then near this point Eq. (D9) may be expanded as

$$Z_c + \Delta \approx (p_c+\epsilon)[1 - (1-f)G_1(1-Z_c) + G_2(1-Z_c)\Delta - S_3(1-Z_c)\Delta^2], \tag{D12}$$

which gives

$$\Delta \approx \frac{1-(1-f)G_1(1-Z_c)}{1-p_cG_2(1-Z_c)}\epsilon \tag{D13}$$

for $\epsilon \ll 1$, where higher-order terms have been neglected.

Similarly, for Y we note that, since δ is zero at the critical point, $Y_c = Z_c$. So

$$Y = Z - \delta = Z_c + \Delta - \delta \tag{D14}$$

near the threshold. This means we can use the expansion Eq. (D12), as well as Eqs. (D6) and (D7) for Y, by substituting $\Delta - \delta$ for Δ.

We first expand Eq. (D11) to leading orders of X:

$$\delta \approx p[G_2(1)X - G_3(1)X^2] - p(1-f)\Big[G_1(1-Z) - G_1(1-Y) + G_2(1-Y)X - \frac{1}{2}G_3(1-Y)X^2\Big]. \tag{D15}$$

Then we have to expand the generating functions, which are functions of $1-Z$ and $1-Y$ in Δ and $\Delta-\delta$, respectively. Since $Z_c = Y_c$, a few terms cancel, and we get, neglecting all terms that are second order in small values,

$$\delta \approx pG_2(1)X - p(1-f)G_1(1-Z_c)(X-\delta), \tag{D16}$$

which can be rearranged to give

$$\delta \approx \frac{pG_2(1) - p(1-f)G_2(1-Z_c)}{1-p(1-f)G_2(1-Z_c)}X. \tag{D17}$$

We still have not considered these expansions in terms of the deviation of p from the critical value p_c. We will come to this later.

Now that we have worked out the expansions of all the "secondary" quantities, we are finally ready to consider the behavior of X above the critical point. First we expand the right-hand side of Eq. (D8) in powers of X:

$$X \approx G_2(1)X - \frac{1}{2}G_3(1)X^2 - (1-p)(1-f)\Big[G_1(1-Z) - G_1(1-Y) + G_2(1-Y)X - \frac{1}{2}G_3(1-Y)X^2\Big]. \tag{D18}$$

Then we substitute the expansions for $G_n(1-Z)$ and $G_n(1-Y)$ about Z_c, using Eqs. (D6) and (D7):

$$X \approx G_2(1)X - \frac{1}{2}G_3(1)X^2 - (1-p)(1-f) \times \Big\{G_2(1-Z_c)(X-\delta) + \frac{1}{2}G_3(1-Z_c) \times [\Delta^2 - (\Delta-\delta)^2 - 2X(\Delta-\delta) - X^2]\Big\}, \tag{D19}$$

where we have truncated any terms of higher order than $O(X^2)$ or equivalent.

We first use this expression to obtain the criterion for the critical point. Keeping only terms linear in X, substituting the right-hand side of Eq. (D17) for δ, dividing by X, and taking the limit $p \to p_c$ ($X \to 0^+$), we have

$$1 = G_2(1) - (1-p_c)(1-f)G_2(1-Z_c) \times \left\{\frac{1-p_cG_2(1)}{1-p_c(1-f)G_2(1-Z_c)}\right\}, \tag{D20}$$

which is Eq. (13).

Now, to find the behavior of X just above this transition point, we write $p = p_c + \epsilon$ in Eq. (D19). For the sake of brevity, we write the right-hand side of Eq. (D17) as cX and the right-hand side of Eq. (D13) as $d\epsilon$. Then

$$X \approx G_2(1)X - \frac{1}{2}G_3(1)X^2 - (1-p_c-\epsilon)(1-f) \times \Big\{G_2(1-Z_c)(1-c)X + \frac{1}{2}G_3(1-Z_c) \times [d^2\epsilon^2 - (d\epsilon - cX)^2 - 2X(d\epsilon - cX) - X^2]\Big\}. \tag{D21}$$

Using Eq. (D20), removing the common factor X, and rearranging, we find

$$X \cong \frac{2(1-f)(1-c)[(1-p_c)G_3(1-Z_c)d + G_2(1-Z_c)]}{[G_3(1) - (1-p_c)(1-f)G_3(1-Z_c)(1-c)^2]}\epsilon, \tag{D22}$$

where

$$1 - c = \left\{\frac{1-p_cG_2(1)}{1-p_c(1-f)G_2(1-Z_c)}\right\}, \tag{D23}$$

$$d = \frac{1-(1-f)G_1(1-Z_c)}{1-p_cG_2(1-Z_c)}. \tag{D24}$$

Thus, X grows linearly with the distance above the critical point.

Expanding Eq. (4) in $X \ll 1$, we find

$$S \approx \sum_q P(q)\{qX - (1-f)q(1-Y)^{q-1}(X-\delta)\}, \tag{D25}$$

where we have used that $Z = Y + \delta$. Writing the right-hand side of Eq. (D17) as gX, we have

$$S \approx X\sum_q qP(q)\{1-(1-f)q(1-Y)^{q-1}(1-g)\}. \tag{D26}$$

In other words, S is proportional to X near the critical point, so that, from Eq. (D22), we can conclude that

$$S \propto \epsilon = (p - p_c) \tag{D27}$$

near the critical point.

[1] R. M. Anderson, B. Anderson, and R. M. May, *Infectious Diseases of Humans: Dynamics and Control* (Oxford University Press, Oxford, 1992)

[2] M. J. Keeling and K. T. Eames, Networks and epidemic models, J. R. Soc., Interface **2**, 295 (2005).

[3] R. Pastor-Satorras, C. Castellano, P. Van Mieghem, and A. Vespignani, Epidemic processes in complex networks, Rev. Mod. Phys. **87**, 925 (2015).

[4] R. Pastor-Satorras and A. Vespignani, Epidemic Spreading in Scale-Free Networks, Phys. Rev. Lett. **86**, 3200 (2001).

[5] M. Boguñá and R. Pastor-Satorras, Epidemic spreading in correlated complex networks, Phys. Rev. E **66**, 047104 (2002).

[6] G. Baxter and G. Timár, Degree dependent transmission rates in epidemic processes, J. Stat. Mech.: Theor. Expt. (2021) 103501.

[7] R. J. Pais and N. Taveira, Predicting the evolution and control of the COVID-19 pandemic in Portugal, F1000Research **9**, 283 (2020).

[8] T. Yamana, S. Pei, and J. Shaman, Projection of covid-19 cases and deaths in the US as individual states re-open May 4, 2020, MedRxiv (2020).

[9] M. E. J. Newman, Spread of epidemic disease on networks, Phys. Rev. E **66**, 016128 (2002).

[10] E. Kenah and J. M. Robins, Network-based analysis of stochastic SIR epidemic models with random and proportionate mixing, J. Theor. Biol. **249**, 706 (2007).

[11] J. C. Miller, Epidemic size and probability in populations with heterogeneous infectivity and susceptibility, Phys. Rev. E **76**, 010101(R) (2007).

[12] T. Rogers, Assessing node risk and vulnerability in epidemics on networks, Europhys. Lett. **109**, 28005 (2015).

[13] J. C. Miller, Epidemics on networks with large initial conditions or changing structure, PLoS One **9**, e101421 (2014).

[14] Z.-L. Hu, J.-G. Liu, G.-Y. Yang, and Z.-M. Ren, Effects of the distance among multiple spreaders on the spreading, Europhys. Lett. **106**, 18002 (2014).

[15] Z. Su, C. Gao, J. Liu, T. Jia, Z. Wang, and J. Kurths, Emergence of nonlinear crossover under epidemic dynamics in heterogeneous networks, Phys. Rev. E **102**, 052311 (2020).

[16] F. Radicchi and G. Bianconi, Epidemic plateau in critical susceptible-infected-removed dynamics with nontrivial initial conditions, Phys. Rev. E **102**, 052309 (2020).

[17] R. Schlickeiser and M. Kröger, Analytical solution of the SIR-model for the temporal evolution of epidemics: part b. semi-time case, J. Phys. A **54**, 175601 (2021).

[18] P. Krapivsky, Infection process near criticality: influence of the initial condition, J. Stat. Mech.: Theor. Expt. (2021) 013501.

[19] T. Hasegawa and K. Nemoto, Outbreaks in susceptible-infected-removed epidemics with multiple seeds, Phys. Rev. E **93**, 032324 (2016).

[20] G. J. Baxter, S. N. Dorogovtsev, A. V. Goltsev, and J. F. F. Mendes, Bootstrap percolation on complex networks, Phys. Rev. E **82**, 011103 (2010).

[21] G. J. Baxter, S. N. Dorogovtsev, A. V. Goltsev, and J. F. F. Mendes, Heterogeneous k-core versus bootstrap percolation on complex networks, Phys. Rev. E **83**, 051134 (2011).

[22] W. Goffman and V. A. Newill, Generalization of epidemic theory: An application to the transmission of ideas, Nature (London) **204**, 225 (1964).

[23] H. S. Rodrigues, Application of SIR epidemiological model: new trends, Int. J. Appl. Math. Inf. **10**, 92 (2016).

[24] P. Grassberger, On the critical behavior of the general epidemic process and dynamical percolation, Math. Biosci. **63**, 157 (1983).

[25] G. Machado, Threshold generalization of a contagion model on complex networks, Master's thesis, Faculty of Sciences, University of Porto, Portugal, 2019, https://hdl.handle.net/10216/125655.

[26] C. Castellano and R. Pastor-Satorras, On the numerical study of percolation and epidemic critical properties in networks, Eur. Phys. J. B **89**, 243 (2016).